Formation of Trimer and Dimer Radical Cations of Methyl-Substituted Benzenes in γ-Irradiated Low-Temperature Matrices

Kazumasa Okamoto, Shu Seki,* and Seiichi Tagawa*

The Institute of Scientific and Industrial Research, Osaka University, 8-1 Mihogaoka, Ibaraki, Osaka 567-0047, Japan

Received: March 13, 2006; In Final Form: May 15, 2006

Dimer and trimer radical cations of benzene, toluene, and xylenes were produced selectively after γ-irradiation in low-temperature 2-methylpentane matrices with electron scavengers: oxygen (O_2) and *sec*-butyl chloride (*sec*-BuCl). The charge resonance (CR) band of the trimer radical cation (M_3^+) produced via the corresponding dimer radical cation (M_2^+) is clearly seen in the solution containing O_2 as the temperature increases over a range from 80 to 90 K. In *o*-xylene solution, a fairly strong and distinct M_3^+ CR absorption is observed; this is due to the large M_3^+/M_2^+ relative extinction coefficient. All benzene derivatives show an equilibrium between dimer and trimer radical cations at $\sim$ 90 K; however, the equilibrium constants of toluene and the xylenes are considerably lower than that of benzene. Formation of the trimer radical cation is inhibited in *sec*-BuCl, which has commonly been used as a low-temperature optical matrix for producing cationic species. An ab initio DFT method is applied to predict the geometry of M_3^+, giving "slipped sandwich" (for benzene, *m*-xylene, and *p*-xylene) and "slipped fan-shaped" (toluene and *o*-xylene) structures as the most plausible geometries. The experimentally observed spectroscopic parameters reflect well those predicted by TD-DFT calculation based on geometry, suggesting strong dependence of the geometry of M_3^+ on substitution patterns. This is the first report not only of direct spectroscopic observation of aromatic trimer radical cations in the condensed phase but also on the quantitative analysis of their equilibria.

Introduction

The radical cation of benzene forms a dimeric configuration in which charge is localized between two benzene molecules. The evidence has been investigated by ESR[1,2] and by spectroscopic methods such as γ-irradiation at low temperature,[3−10] pulse radiolysis,[11] laser photolysis[12−15] and photodissociation of cluster cations.[16−18] In spectroscopic studies, the charge resonance band (CR band), which corresponds to the transition of a π-electron between the bonding and antibonding state of the dimer radical cation, is observed in the near-infrared (IR) region. In addition, the electronic structure of the benzene dimer radical cation has recently been investigated based on theoretical calculations.[19−24] Radical cations of benzene are also used as a medium of hole transfer to a dielectric polymer.[25−27]

In the condensed phase, some studies on multimer radical cations ($n > 3$) of aromatic molecules such as coronene, naphthalene and biphenyl have been reported.[24,28,29] Benzene aggregate cations ($n > 3$) have been investigated using photodissociation experiments in gas phase.[16] We previously reported the formation of a trimer radical cation of benzene (Bz_3^+) in γ-irradiated 2-methylpentane (2-MP) matrices.[10] The CR band attributed to Bz_3^+ ($\approx$1400 nm) was observed to have an isosbestic point with the dimer radical cation of benzene (Bz_2^+) ($\approx$900 nm) as the temperature was increased from 82 to 85 K. The shift of absorption maxima in the matrices is different from that in the gas phase, in which absorption maxima show a slight shift between Bz_2^+ and Bz_3^+. A dimer ion core model is proposed in the gas phase;[16] however, the configuration of the ion core seems to change depending on high viscosity or a thermal effect in the matrices as the temperature changes from 82 to 85 K. Calculation of the electronic state of Bz_3^+ by the DFT method suggests charge delocalization among the three molecules.

In this work, we have investigated the radical cations of methyl-substituted benzene derivatives in γ-irradiated 2-MP. The absorption spectra were measured by precisely controlling the temperature as the matrix viscosity was loosened. Because 2-MP is a solvent in which both cation and anion species are produced, electron scavengers were added to the solutions. Oxygen (O_2) is an effective electron scavenger which does not have any serious optical effects on the system.[10] Alkyl halides have also been commonly used as scavengers. The dependence of absorption on the type of scavenger present was studied. The electronic states and configurations of the dimer radical cation and trimer radical cation are discussed based on DFT calculations. These studies may provide important insights into the nature of charged benzene aggregates.

Experimental Section

Sample solutions in 2.0 mm thick Suprasil quartz cells were bubbled with O_2 gas (> 99.99%) for 5 min. The solutions were frozen rapidly under liquid N_2, and irradiated by γ-rays from a ^{60}Co source for 1 h at the Institute of Scientific and Industrial Research, Osaka University. The dose rate was 4 kGy/h. The samples were transferred into an Oxford Optistat DN cryostat with flat sapphire windows. The temperature was raised from

* Corresponding authors. (S.S.) E-mail: seki@sanken.osaka-u.ac.jp. Telephone: +81-6-6879-8502. Fax: +81-6-6876-3287. (S.T.) E-mail: tagawa@sanken.osaka-u.ac.jp. Telephone: +81-6-6879-8500. Fax: +81-6-6876-3287.

10.1021/jp061527m CCC: $33.50
Published on Web 06/15/2006

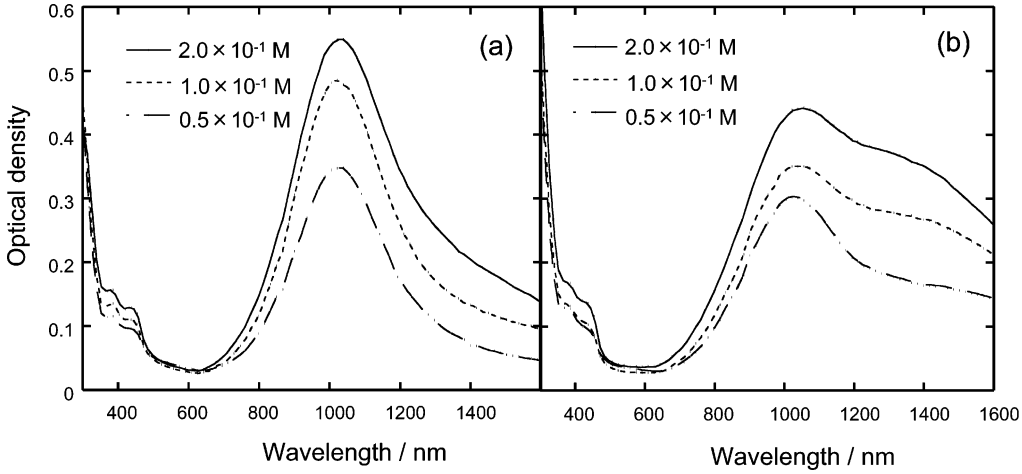

Figure 1. Absorption spectra of 2.0×10^{-1} M, 1.0×10^{-1} M, and 0.5×10^{-2} M toluene in 2-MP with O_2. The spectra were recorded at 82 K (a) and 86 K (b).

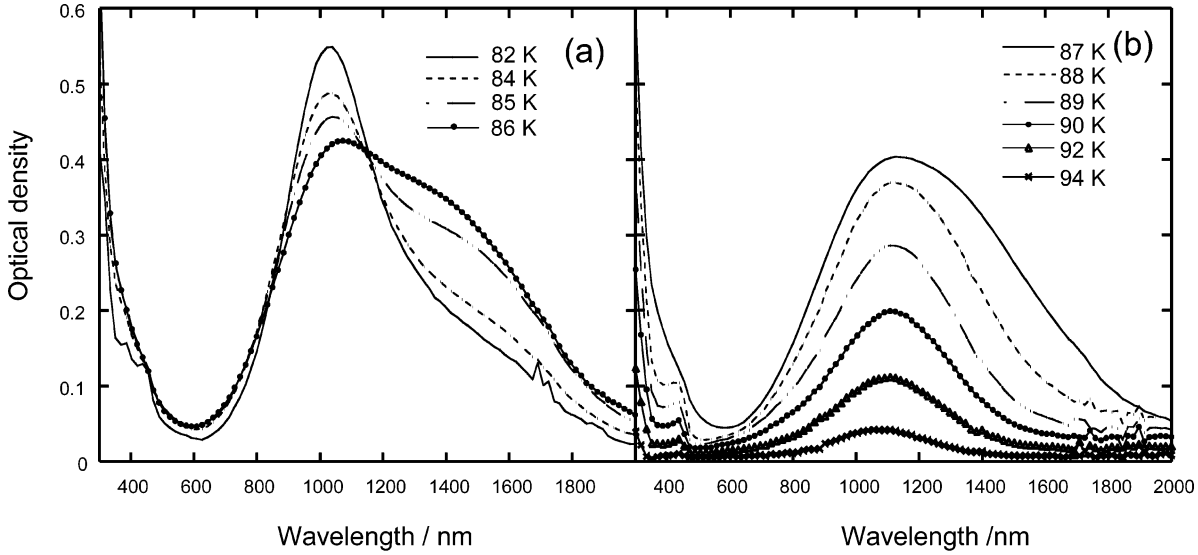

Figure 2. Absorption spectra of 2.0×10^{-1} M toluene in 2-MP with O_2 at (a) 84−87 K and (b) 88−94 K after γ-irradiation.

80 K with a slow heating rate (<0.4 K/min), and was stabilized within ±0.1 K for at least 2 min before each measurement. Absorption spectra were recorded using a UV-3100PC (Shimadzu, 300−2000 nm) spectrophotometer. Details of the set of apparatus used are described elsewhere.[30] Reagents were purchased from Aldrich. Benzene (99.9%), *o*-xylene (98%), *m*-xylene (99%), *p*-xylene (99%), 2-MP (99%), and *sec*-butyl chloride (*sec*-BuCl) were used as received. Toluene (99.8%) was used after reflux distillation.

Results and Discussion

(1) Absorption Spectra of Benzene Derivatives in 2-Methylpentane. Figure 1 shows the absorption spectra of O_2-saturated toluene solutions in γ-irradiated 2-MP at 82 K. The dissolved O_2 scavenges electrons, with the result that formation of radical solute anions is suppressed in the matrices.[10] These spectra show a large characteristic absorption band at 1040 nm in the near-IR region with a small shoulder at 440 nm. Absorption bands in near-IR region are assigned to the charge resonance (CR) band of the dimer radical cation (M_2^+), as reported for benzene and its derivative solutions.[4−13] The absorption maximum (1040 nm) shows good agreement in 3-methylpentane,[5a,6,7] CCl_4,[5b,d] and C_4H_9Cl[5c] glasses at 77 K, and it is slightly red-shifted in contrast with that of a γ-irradiated *n*-butyl chloride and isopentane mixture at 77 K (926 nm).[4] This difference is probably due to variation in experimental conditions, such as solvents and temperature. The CR band is enhanced as the concentration of toluene is increased at 82 K. This dependence has been reported as one proof for the formation of M_2^+. The absorption at 440 nm, which shows similar concentration dependence to the CR band, is assigned similarly to the local excitation (LE) band of M_2^+.[18] New absorption bands are observed around 1400 nm as the temperature increases, as shown in Figure 2. The absorption band is emphasized as the toluene concentration is increased. Figure 2 shows a clear isosbestic point between the CR band of M_2^+ and the new absorption at 82−85 K. The decrease of the CR band and the new absorption due to recombination of O_2^- anions becomes clear above 86 K. It is suggested that intermediates with absorption at ≈ 1400 nm increase with consumption of M_2^+. We can also see the disappearance of the new band above 86 K with spectral shift of M_2^+. We assigned the band at ≈ 1400 nm to the CR band of M_3^+ of toluene (T_3^+), as reported previously in benzene-2MP solution, in which an isosbestic point between Bz_2^+ and Bz_3^+ is also observed clearly.[10] The disappearance of the band above 86 K is suggestive of a change in equilibrium with increasing temperature or transformation to other intermediates. The reaction mechanism in the γ-irradiated

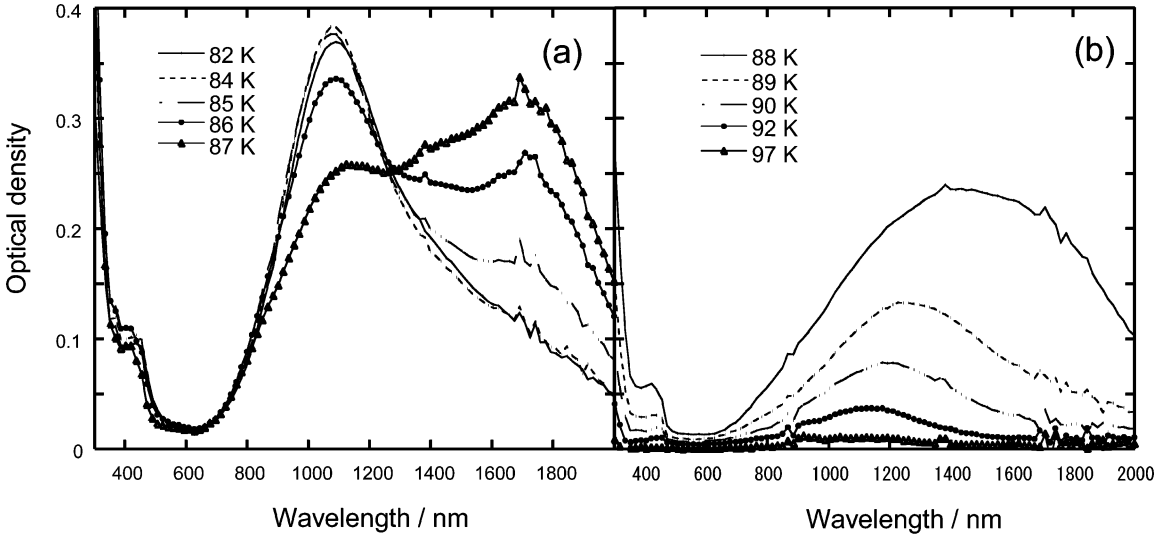

Figure 3. Absorption spectra of 2.0×10^{-1} M *o*-xylene in 2-MP with O_2 at (a) 84−87 K and (b) 88−94 K after γ-irradiation.

TABLE 1: Absorption Maxima of CR Bands of M_2^+ and M_3^+, Ratios of O.D. (M_3^+/M_2^+), Ratios of Extinction Coefficient Maxima ($\epsilon[M_3^+]_{Max}/\epsilon[M_2^+]_{Max}$) and Equilibrium Constants between M_3^+ and M_2^+, with Calculated Values for Maximum Absorption (λ_{Max}^{TD}) and Relative Oscillator Strength (f_2/f_3) by TD-DFT

	λ_{max}/nm					λ_{max}^{TD}/nm		
entry	M_2^+	M_3^+	O.D.$[M_3^+]$/O.D.$[M_2^+]$ [e]	$\epsilon[M_3^+]_{max}/\epsilon[M_2^+]_{max}$ [e]	K_4/M^{-1}	M_2^+	M_3^+	f_2/f_3
benzene	930[a]	1380[c]	0.90[c]	1.1[c]	4.1[c]	850	1380	1.0
toluene	1040[a]	1470[c,e]	0.37[c]	2.0[c]	0.9[c]	930	1550	1.6
o-xylene	1090[b]	1740[d]	0.87[d]	3.4[d]	1.3[d]	1030	1790	1.9
m-xylene	1000[b]	1540 [d,e]	0.23[d]	1.1[d]	1.0[d]	960	1640	0.95
p-xylene	1190[b]	1690[d]	0.55[d]	1.6[d]	1.7[d]	1100	1860	1.2

[a] At 82 K. [b] At 84 K. [c] At 86 K. [d] At 87 K. [e] Estimated from differential spectra and Gaussian fitting curves.

matrixes may be summarized as follows:

$$\text{2-MP} \rightsquigarrow \text{2-MP}^+ + e^- \quad (1)$$

$$\text{2-MP}^+ + M \rightarrow M^+ \quad (2)$$

$$M^+ + M \underset{K_3}{\rightleftharpoons} M_2^+ \quad (3)$$

$$M_2^+ + M \underset{K_4}{\rightleftharpoons} M_3^+ \quad (4)$$

$$e^- + O_2 \rightarrow O_2^- \quad (5)$$

$$e^- + M \rightarrow [M]^- \xrightarrow{O_2} M + O_2^- \quad (6)$$

The concentration of O_2 at the saturation was estimated as 15.0 mM at 293 K.[31] It was reported that molecular oxygen and benzene derivatives in 2-MP give the triplet charge-transfer complex ($^3M-O_2$ CT) which showed slight increase in the shoulder of the UV spectra in the range of 300−350 nm.[32] With decrease in temperature down to 77 K, the shoulder band attributed to the $^3M-O_2$ CT formation increased gradually, suggesting an increase in the concentration of O_2 in the low-temperature range. According to the precise analysis of the shoulder band observed for benzene solution in 2-MP at 200 mM concentration, the saturated concentration of O_2 at 77 K was estimated as lower than 25 mM, which was far lower than the benzene concentration in the present cases. Because of this insufficient concentration of the electron scavenger; O_2, initial formation and recombination processes of anionic species of benzene derivatives cannot be neglected though electron affinity of O_2 is far higher than those of all benzene derivatives used in the present study. This may cause the relative decrease in the yield of cationic species in comparison to the yield observed for the case with sufficient electron scavenger. This issue is discussed in the following section.

Absorption spectra were also measured for γ-irradiated *o*-, *m*-, and *p*-xylene solutions. Figure 3 shows the absorption spectra of O_2-saturated 2.0×10^{-1} M solutions of *o*-xylene. These xylene solutions also show CR bands of M_2^+ and M_3^+, the latter of which becomes visible with increasing temperature. We can observe the disappearance of the M_3^+ with spectral shift above 89 K, similar to the toluene solution. These solutions showed spectral change from M_2^+ to M_3^+ at higher temperatures (84 K) compared with benzene and toluene (82 K), although decay of the CR bands due to recombination begins to appear at a similar temperature. The mobility of the counteranions (O_2^-) seems similar in these media; however, benzene and toluene molecules seem to move more easily than the xylene molecules because of their lower steric hindrance. Absorption maxima, ratios of O.D. and extinction coefficients, and equilibrium constants for M_3^+ and M_2^+ (K_4) are summarized in Table 1. K_4 is expressed as follows:

$$\frac{[M_3^+]}{[M_2^+][M]} = K_4 \quad (7)$$

We calculated each K_4 at the temperature at which the optical density of M_3^+ showed a maximum. Below these temperatures, the system does not seem to reach equilibrium because of the hard matrices effect. The wavelength of the absorption maximum of M_2^+ in *m*-xylene solution is good agreement with that reported previously.[4] The K_4 value for each benzene derivative is smaller than the previously reported equilibrium constants of M_2^+ and M^+ (K_3), $10^5 \sim 10^4$ M^{-1}.[3] It is suggested that the stabilization of M_3^+ by charge resonance is similar to that of

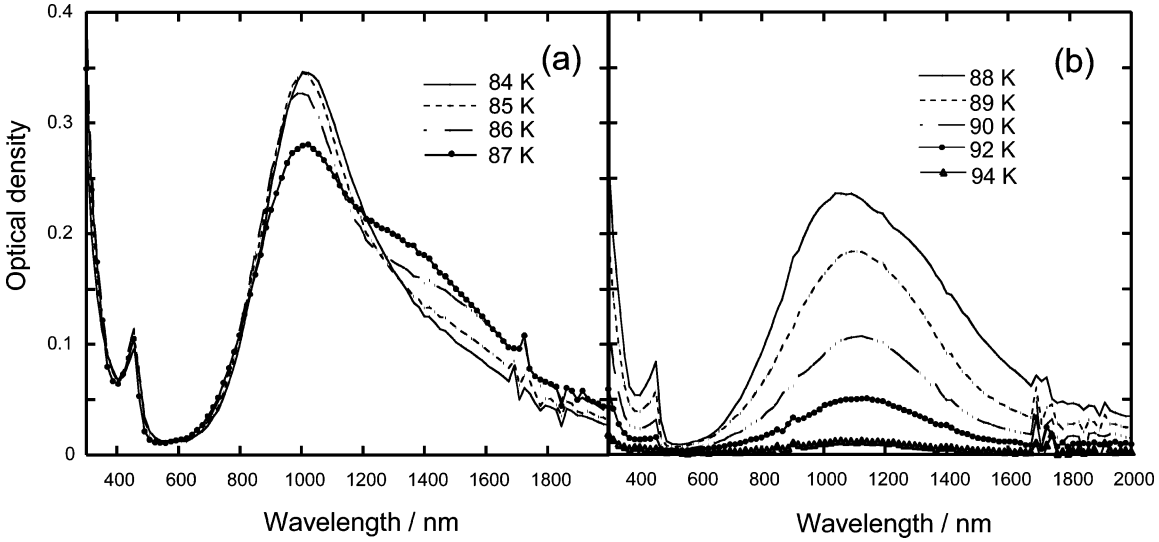

Figure 4. Absorption spectra of 2.0×10^{-1} M *m*-xylene in 2-MP with O_2 at (a) 84−87 K and (b) 88−94 K after γ-irradiation.

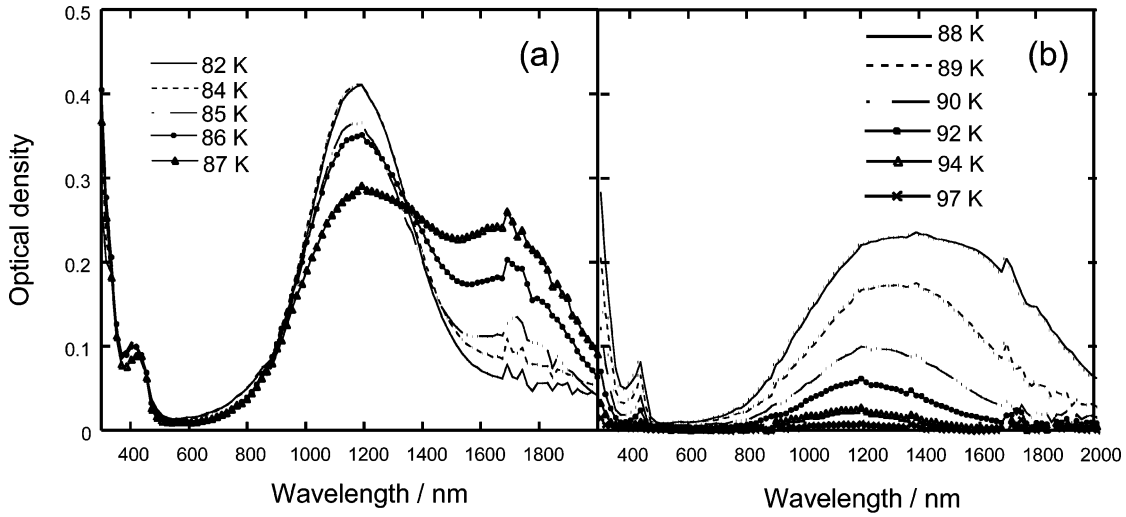

Figure 5. Absorption spectra of 2.0×10^{-1} M *p*-xylene in 2-MP with O_2 at (a) 84−87 K and (b) 88−94 K after γ-irradiation.

M_2^+. The absorption maximum of M_3^+ in *m*-xylene solution is vague even in 2×10^{-1} M solution, whereas that of M_3^+ in *o*-xylene solution is as distinct as that of benzene. This is due to a difference in the ratio of extinction coefficients between M_3^+ and M_2^+. The equilibrium of M_3^+ and M_2^+ of *m*- and *p*-xylenes was also observed in the same low-temperature matrixes as shown in Figures 4 and 5. The absorption maxima, extinction coefficient ratio, and equilibrium constants are estimated and summarized in Table 1. The extinction coefficient ratio of *o*-xylene is calculated to be three times higher than that of *m*-xylene. Therefore, to summarize the above discussion, K_4 is depressed by methyl-substitution.

(2) Absorption Spectra of Benzene Derivatives in γ-Irradiated *sec*-Butyl Chloride Glasses. Alkyl halides have been used, in the form of solvents or additives, as negative charge scavengers to allow the selective production of solute radical cations by ionizing radiation. Electrons are stabilized as halide anions in the matrices or solutions. Radical cations of benzene and its derivatives have also been selectively produced by using alkyl halides.[4−7] However, the CR bands of M_3^+ have not been observed in benzene and methyl-substituted solutions. We carried out absorption spectrum measurements of benzene solutions in *sec*-butyl chloride to elucidate this discrepancy.

Figure 6 shows absorption spectra of benzene solutions in Ar saturated 2-MP with 10 vol % *sec*-BuCl at 82−94 K after γ-irradiation. The spectra show a CR band in the near-IR region, similarly to the O_2-saturated solutions. The absorption maxima are in good agreement with that of Bz_2^+. In comparison to the spectra recorded for O_2-saturated 2-MP without *sec*-butyl chloride, the initial yield of Bz_2^+ shows considerable increase in the case of 2-MP/*sec*-butyl chloride system with 200 mM benzene, giving ∼20 % higher yield of Bz_2^+. However with decrease in the benzene concentration, the difference in the yield was reduced, and almost equivalent yields were observed in both O_2 saturated 2-MP and 2-MP/*sec*-butyl chloride systems with benzene at 50 mM concentrated

One can also observe a new absorption band at 600 nm which was not observed in the O_2-saturated solutions. The LE band of Bz_2^+ is concealed by this chromophore at lower temperatures. The 600 nm band in the visible region was also observed in other benzene derivatives; the observed absorptions are summarized in Table 2. The 600 nm band decreases at a lower temperature than the CR band and LE band of Bz_2^+. As the concentration of benzene is increased, the intensity of the CR band increases, and the CR band disappears gradually with increasing temperature from 86 to 90 K. However, the intensity of the 600 nm band, which is similar in the 0.05 and 0.1 M solutions, is less in the 0.2 M solution. Figure 7 shows the absorption spectra of 0.2 M benzene solutions in 2-MP with 0−10 vol % *sec*-BuCl at 84 K after γ-irradiation. The 600 nm

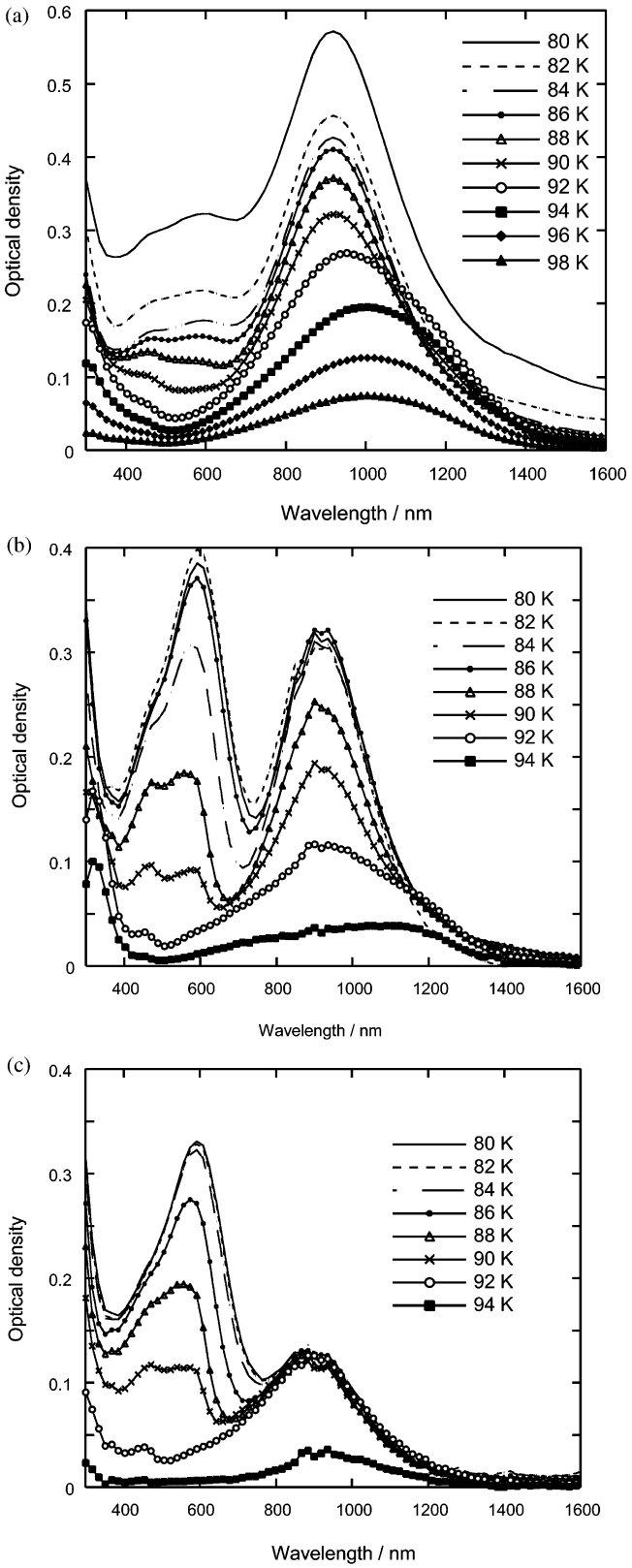

Figure 6. Absorption spectra of (a) 2.0×10^{-1} M, (b) 1.0×10^{-1} M, and (c) 0.5×10^{-2} M benzene solutions in 2-MP with 10 vol % *sec*-BuCl at 82−94 K after γ-irradiation.

band increases as the amount of *sec*-BuCl increases; an isosbestic point is observed between this band and the CR band. It is likely that Bz_2^+ is produced by consumption of the species responsible for the 600 nm band, because the decay of the 600 nm band is faster than that of the CR band. Deducing from the above results, the intermediate chromophore may be identified

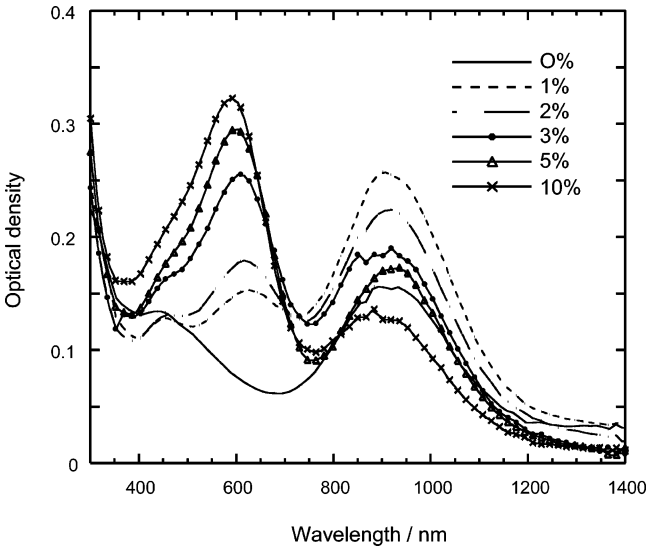

Figure 7. Absorption spectra of 2.0×10^{-1} M benzene solution in 2-MP with 0−10 vol % *sec*-BuCl at 84 K after γ-irradiation.

TABLE 2: Absorption Maxima of CR Bands of Benzene Derivatives in γ-irradiated *sec*-BuCl

	λ_{max}/nm	
	visible	CR band
benzene	470, 590	920
toluene	450, 540	1020
o-xylene	450 490	1090
m-xylene	470, 510	990
p-xylene	420, 450	1160

TABLE 3: Optimized Geometrical Parameters of Dimer and Trimer Radical Cations: Inter-Planar Distances (IPD), Ring Center Displacements (δx and δy), and Rotation and Tilt Angles (θ_{Rot} and θ_{Tl}) of the Ring Planes

entry	IPD (nm)	δx (nm)	δy (nm)	θ_{Rot} (deg)	θ_{Tl} (deg)
$(benzene)_2^+$	0.338	0.0895	0.0134	<0.5	<0.5
$(toluene)_2^+$	0.335	0.0360	0.0100	<0.5	1.0
$(o\text{-xylene})_2^+$	0.339	0.1068	0.0036	<0.5	1.0
$(m\text{-xylene})_2^+$	0.334	0.1027	0.0697	6.0	6.8
$(p\text{-xylene})_2^+$	0.344	0.1092	0.0016	<0.5	<0.5
$(benzene)_3^+$	0.352	0.0517	0.0914	1.8	1.8
$(toluene)_3^+$	0.353	0.0142	0.1277	23.4	12.7
$(o\text{-xylene})_3^+$	0.359	0.1130	0.1130	19.9	2.5
$(m\text{-xylene})_3^+$	0.353	0.1015	0.0736	2.9	4.4
$(p\text{-xylene})_3^+$	0.368	0.1102	0.0273	1.7	<0.5

as an ionic complex $(MA)^+$ in which aromatics and *sec*-butyl chloride share one positive charge. It may be concluded that the reaction mechanism after positive charge transfer from solvent to solute is as follows:

$$M^{\bullet +} + A \rightarrow \underset{\text{(ionic complex)}}{(MA)^{\bullet +}} \overset{-M}{\rightleftharpoons}$$

$$M^{\bullet}{}_2^{+} + A \overset{-M}{\rightleftharpoons} M^{\bullet}{}_3^{+} + A \quad (8)$$

Similar types of complexes between aromatic monomer cations and alkyl halides have previously been proposed.[7,28] Thus, the presence of alkyl halides may obscure the trimer radical cation, because the reaction equilibrium favors the monomer cation complex. Absorption of Bz_3^+ is suppressed due to the formation of the stabilized complex.

(3) Structure of Trimer and Dimer Radical Cation of Benzene Derivatives. Geometrical optimization of the dimer and trimer radical cations of benzene derivatives was performed

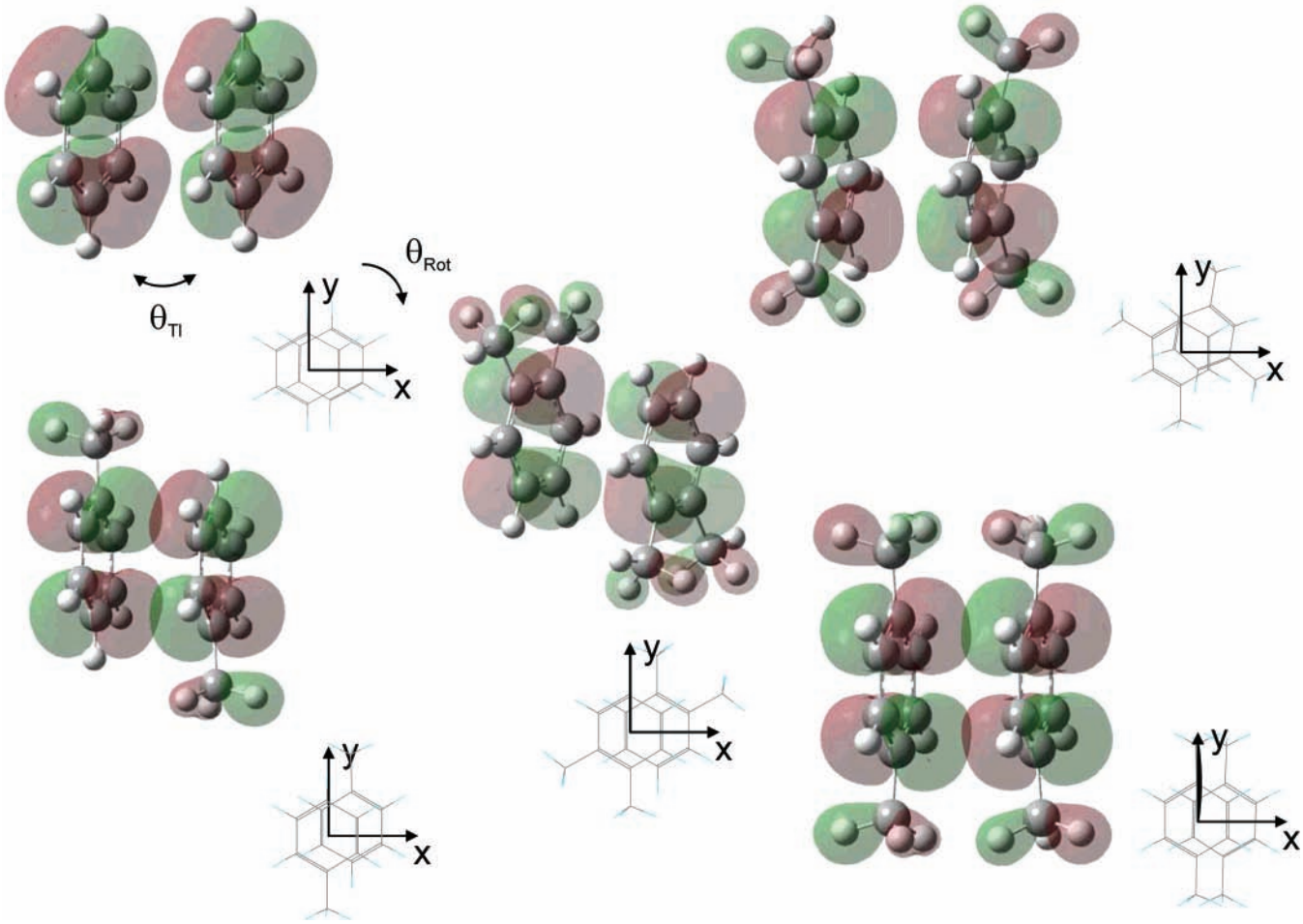

Figure 8. Optimized geometry of dimer radical cations of benzene derivatives with tron density maps of singly occupied molecular orbitals. The Cartesian coordinates are defined as the ring-diagonal vector of each respective "front" ring in the dimer cation radical.

in this study by the DFT method. The optimized structures of the dimers and trimers, obtained by B3LYP/6-31G+(d,p) calculations, are displayed in Figures 8 and 9, respectively, with electron density maps of the singly occupied molecular orbitals. On the basis of the Cartesian coordinates represented in the figures, the structures of the dimers and the trimers are analyzed quantitatively. Displacement of the geometrical centers of the benzene rings from the corresponding complete parallel stacking structures are defined relative to the center of the "front" ring (dimer) or to the "central" ring (trimer) as δx and δy along the Cartesian axis. The "tilt" and "rotation" angles of the ring-planes are defined as the angles of the ring-diagonal vectors projected into $y-z$ (θ_{Tl}) and $x-y$ (θ_{Rot}) planes, respectively. The optimized geometric parameters of the structures are summarized in Table 3. The dimers of benzene, toluene, *o*-xylene, and *p*-xylene show "slipped parallel" structures (stacking of the distorted benzene rings with some displacement in both x (δx) and y (δy) directions); however, a rotated and tilted ring form is considered the most plausible structure for the *m*-xylene dimer radical cation. Repulsive interactions between methyl substituents seem to be dominant in toluene, *o*-xylene, and *m*-xylene, but attracting forces give a certain stabilization to the dimer of *p*-xylene because of the considerable difference in electron density in the methyl substituents. The interplanar distances (IPDs) of the dimers are distributed between 0.334 and 0.344 nm for all dimer radical cations. The values of IPD, δx, and δy in the "slipped parallel" structure of the benzene radical cation shows good agreement with the forms suggested by other theoretical calculations.[2,23b]

In contrast to the structures of the dimer radical cations, the trimers of toluene and *o*-xylene show larger values of θ_{Tl} and θ_{Rot} compared to those calculated for the benzene, *o*-xylene, and *p*-xylene trimer radical cations, which have slipped sandwich structures with small values of θ_{Tl}. The slipped parallel structure of the benzene trimer radical cation was reported as a C_2v structure with $\delta x = \pm 0.114$ nm and IPD = 0.366 nm based on the CASSCF and MRSDCI methods,[22b] and this structure was supported by the ^{1}H hyperfine splitting constants of chemically oxidized coronene radical cations as observed by ESR spectroscopy.[24] The toluene and *o*-xylene trimer radical cations have peculiar global geometries, as shown in Figure 9. The planes of the three rings are no longer "sandwiched", and the larger values of θ_{Tl} and θ_{Rot} seem to induce "slipped fan-shaped" or helical structures. This may be the reason for the considerable rise in the molar extinction coefficient of M_3^+ observed for *o*-xylene.

On the basis of the optimized geometry of the dimer and trimer radical cations of the benzene derivatives, optical transition energy and oscillator strength were calculated by the time-dependent (TD) DFT method with 6-311+G(d,p) basis functions. The values are summarized in Table 1 along with the experimentally observed values of absorption maxima and molar extinction coefficients. The changes in transition energies of the dimers and trimers show similar trends both experimentally and theoretically, with disagreement smaller than 0.13 eV. The relative values of extinction coefficients and the oscillator strengths also reflect the experimentally obtained values, except for *o*-xylene, whose experimental extinction coefficient ratio is

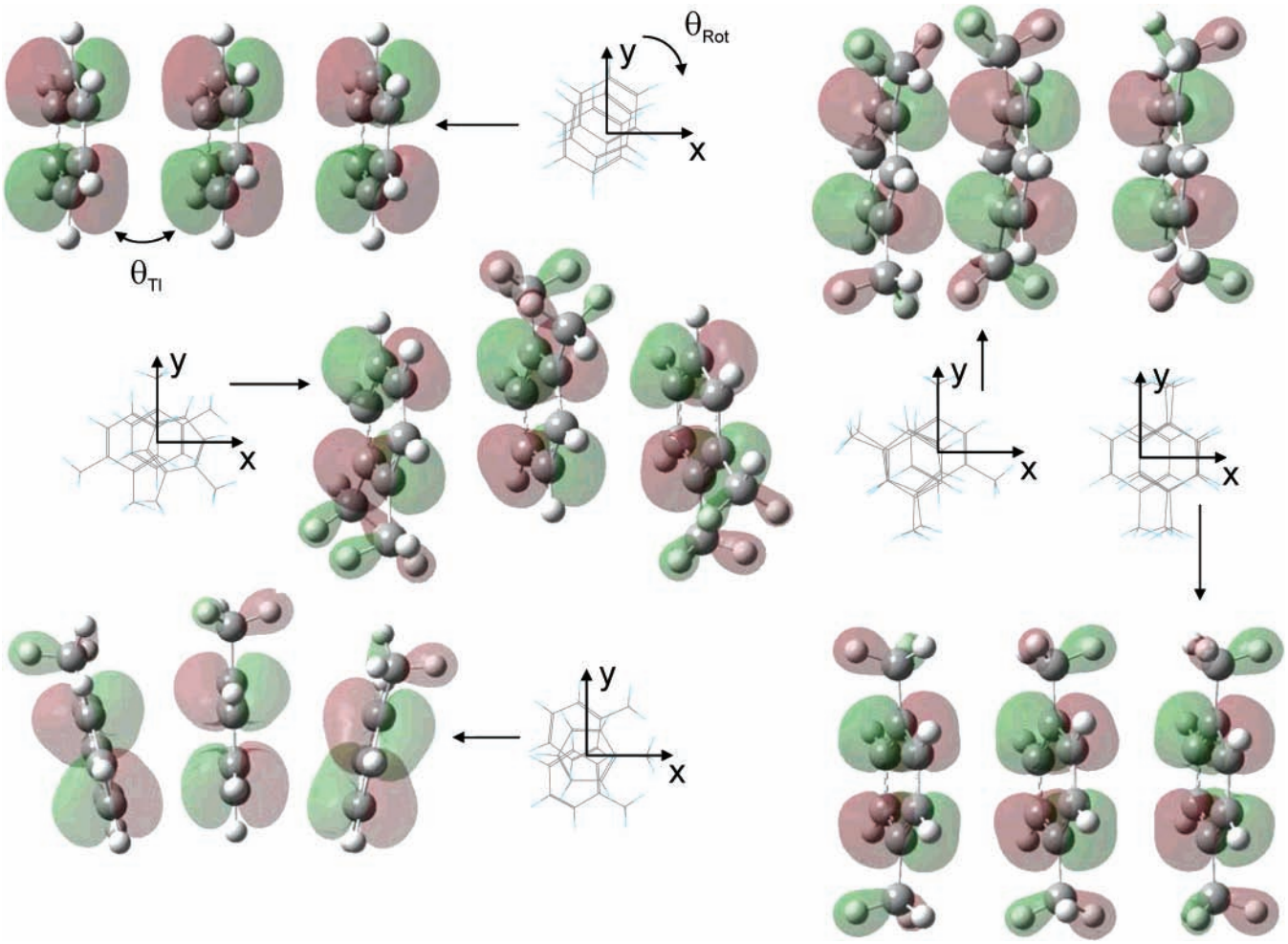

Figure 9. Optimized geometry of trimer radical cations of benzene derivatives with tron density maps of singly occupied molecular orbitals. The Cartesian coordinates are defined as the ring-diagonal vector of each respective "center" ring in the trimer cation radical.

extremely high. Another minimum conformer may be found for *o*-xylene, but so far we have not detected any.

The concentration of dimer radical cations formed in the matrices can be estimated using the calculated values of oscillator strength and extinction coefficient for the transients. The absorption intensity attributed to the dimer radical cations suggests that the dimer yield G(dimers) = 0.15−0.24 (100 eV)$^{-1}$ for all the benzene derivatives. This value corresponds to the previously reported free ion yield (G_{fi} = 0.17−0.21) in 2-MP,[33] which demonstrates the high reliability of the structures and optical properties calculated in the present study.

Conclusion

CR optical absorptions of trimer radical cations (M_3^+) were successfully observed for benzene derivatives in low-temperature 2-MP matrices by γ-radiolysis. In particular, the CR band of M_3^+ was observed clearly and distinctly for *o*-xylene as well as the M_3^+ of benzene. This is due to the large extinction coefficient of M_3^+ relative to that of M_2^+. All the benzene derivatives examined in the present study were in equilibrium between trimer and dimer radical cations at ∼ 90 K; however, the equilibrium constants of methyl-substituted benzene derivatives were $^1/_3$−$^1/_4$ of that of benzene. It is likely that methyl substitution has a steric effect on the formation of M_3^+. In contrast, formation of trimer radical cations was not observed in a *sec*-BuCl matrix, because γ-radiolysis of the matrix resulted in the formation of a complex between the cations and Cl^-. Geometrical optimization of M_2^+ and M_3^+ was performed using an ab initio DFT method, and "slipped parallel" structures were suggested for the M_2^+ species of all benzene derivatives. However, plausible structures for the M_3^+ species depended strongly on substitution patterns, with "slipped sandwich" structures deduced for benzene, *m*-xylene, and *p*-xylene, but "slipped fan-shaped" structures for toluene and *o*-xylene. The spectroscopic properties of M_2^+ and M_3^+ predicted by TD-DFT calculation provide good interpretations of the transient spectra observed in the present study.

References and Notes

(1) Edlund, O.; Kinell, P. O.; Lund, A.; Shimizu, A. *J. Chem. Phys.* **1967**, *46*, 3679−3680.

(2) Itagaki, Y.; Benetis, N. P.; Kadam, R. M.; Lund, A. *Chem. Phys. Phys. Chem.* **2000**, *46*, 2683−2689.

(3) Badger, B.; Brocklehurst, B. *Nature (London)* **1968**, *219*, 263.

(4) Badger, B.; Brocklehurst, B. *Trans. Faraday Soc. 2* **1969**, *65*, 2582−2587.

(5) (a) Guarino, J. P.; Hamill, W. H. *J. Am. Chem. Soc.* **1964**, *86*, 777−781. (b) Shida, T.; Hamill, W. H. *J. Chem. Phys.* **1966**, *44*, 2375−2377. (c) Shida, T.; Hamill, W. H. *J. Chem. Phys.* **1966**, *44*, 4372−4377. (d) Louwrier, P. W. F.; Hamill, W. H. *J.* Phys. Chem. **1969**, *73*, 1707−1711. (e) Shida, T. *Electronic absorption spectra of radical ions*; Elsevier: Amsterdam, 1988.

(6) Ekstrom, A. *J. Phys. Chem.* **1970**, *74*, 1705−1708.

(7) Bühler, R. E.; Funk, J. *J. Phys. Chem.* **1975**, *79*, 2098−2105.

(8) Miller, J. H.; Andrews, L.; Lund, P. A.; Schhatz, P. N. *J. Chem. Phys.* **1980**, *73*, 4932−4939.

(9) Schroeter, K.; Schröder, D.; Schwarz, H.; Reddy, G. D.; Wiest, O.; Carra, C.; Bally, T. *Chem.—Eur. J.* **2000**, *6*, 4422−4430.

(10) Todo, M.; Okamoto, K.; Seki, S.; Tagawa, S. *Chem. Phys. Lett.* **2004**, *399*, 378−383.

(11) Okamoto, K.; Saeki, A.; Kozawa, T.; Yoshida, Y.; Tagawa, S. *Chem. Lett.* **2003**, *32*, 834−835.

(12) Tagawa, S.; Beck, G.; Schnabel, W. *Z. Naturforsch.* **1982**, *37a*, 982−984.

(13) (a) Schlief, R. E.; Jarzeba, W.; Barbara, P. F. *J. Phys. Chem.* **1994**, *98*, 9102−9105. (b) Schlief, R. E.; Jarzeba, W.; Thakur, K. A. M.; Alfano, J. C.; Johnson, A. E.; Barbara, P. F. *J. Mol. Liq.* **1994**, *60*, 201−220.

(14) (a) Ojima, S.; Miyasaka, H.; Mataga, N.*J. Phys. Chem.* **1990**, *94*, 4147−4152. (b) Ojima, S.; Miyasaka, H.; Mataga, N. *J. Phys. Chem.* **1990**, *94*, 5834−5839. (c) Ojima, S.; Miyasaka, H.; Mataga, N. *J. Phys. Chem.* **1990**, *94*, 7534−7539.

(15) Inokuchi, Y.; Naitoh, Y.; Ohashi, K.; Saitow, K.; Yoshihara, K,; Nishi, N. *Chem. Phys. Lett.* **1997**, *269*, 298−304.

(16) Krause, H.; Ernstberger, B.; Neusser, H. J. *Chem. Phys. Lett.* **1991**, *184*, 411−417.

(17) Beck, S. M.; Hecht, J. H.*J. Chem. Phys.* **1992**, *96*, 1975−1981.

(18) (a) Ohashi, K.; Nishi, N. *J. Chem. Phys.* **1991**, *95*, 4002−4009. (b) Ohashi, K.; Nishi, N. *J. Chem. Phys.* **1992**, *96*, 2931−2932. (c) Shibata, T.; Ohashi, K.; Nakai, Y.; Nishi, N. *Chem. Phys. Lett.* **1994**, *229*, 604−608. (d) Nakai, Y.; Ohashi, K.; Nishi, N. *J. Phys. Chem. A* **1997**, *101*, 472−480.

(19) Milosevich, S. A.; Saichek, K.; Hinchey, L.; England, W. B.; Kovacic, P. *J. Am. Chem. Soc.* **1983**, *105*, 1088−1090.

(20) Hiraoka, K.; Fujimaki, S.; Aruga, K. *J. Chem. Phys.* **1991**, *95*, 8413−8418.

(21) Kadam, R. M.; Itagaki, Y.; Erickson, R.; Lund, A. *J. Phys. Chem. A* **1999**, *103*, 1480−1486.

(22) (a) Miyoshi, E.; Ichikawa, T.; Sumi, T.; Sakai, Y.; Shida, N. *Chem. Phys. Lett.* **1997**, *275*, 404−408. (b) Miyoshi; E. Ghosh; T. K. *Chem. Phys. Lett.* **2000**, *323*, 434−440.

(23) (a) Rusyniak, M. J.; Ibrahim, Y. M.; Wright, D. L.; Khanna, S. N.; El-Shall, M. S. *J. Am. Chem. Soc.* **2003**, *125*, 12001−12013. (b) Ibrahim, Y.; Alsharaeh, E.; Rusyniak, M.; Watson, S.; Meot-Ner, M.; El-Shall, M. S. *Chem. Phys. Lett.* **2003**, *380*, 21−28.

(24) Komaguchi, K.; Nomura, K.; Shiotani, M.; Lund, A.; Jansson, M.; Lunell, S. *Spectrochim. Acta A* **2006**, *63A*, 76−84.

(25) Monkman, A. P.; Burrows, H. D.; Hartwell, L. J.; Horsburgh, L. E.; Hamblett, I.; Navaratnam, S. *Phys. Rev. Lett.* **2001**, *86*, 1358−1361.

(26) (a) Candeias, L. P.; Grozema, F. C.; Padmanaban, G.; Ramakrishnan, S.; Siebbeles, L. D. A.; Warman, J. M.*J. Phys. Chem. B* **2003**, *107*, 1554−1558. (b) Grozema, F. C.; Siebbels, L. D. A.; Warman, J. M.; Seki, S.; Tagawa, S.; Scherf, U. *Adv. Mater.* **2002**, *14*, 228−231. (c) Grozema, F. C.; Hoofman, R. J. O. M.; Candeias, L. P.; de Haas, M. P.; Warman, J. M.; Siebbels, L. D. A. *J. Phys. Chem. A* **2003**, *107*, 5976−5986. (d) Candeias, L. P.; Wildeman, J.; Hadzioannou, G.; Warman, J. M. *J. Phys. Chem. B* **2000**, *104*, 8366−8371.

(27) (a) Seki, S.; Koizumi, Y.; Kawaguchi, T.; Habara, H.; Tagawa, S. *J. Am. Chem. Soc.* **2004**, *126*, 3521−3526. (b) Kawaguchi, T.; Seki, S.; Okamoto, K.; Saeki, A.; Yoshida, Y.; Tagawa, S. *Chem. Phys. Lett.* **2003**, *373*, 353−357.

(28) (a) Kira, A.; Nakamura, T.; Imamura, M. *J. Phys. Chem.* **1977**, *81*, 511−516. (b) Kira, A.; Imamura, M. *J. Phys. Chem.* **1979**, *83*, 2267−2273. (c) Kira, A.; Imamura, T.; Shida, T. *J. Phys. Chem.* **1976**, *80*, 1445−1448.

(29) Ohkita, H.; Fushimi, T.; Atsumi, K.; Fujita, Y.; ito, S.; Yamamoto, M. *Chem. Phys. Lett.* **2003**, *374*, 137−142.

(30) (a) Seki, S.; Yoshida, Y.; Tagawa, S.; Asai. K. *Macromolecules* **1999**, *32*, 1080−1086. (b) Seki, S.; Cromack, K. R.; Trifunac, A. D.; Yoshida, Y.; Tagawa, S.; Asai, K.; Ishigure, K. *J. Phys. Chem. B* **1998**, *102*, 8367−8371. (c) Seki, S.; Matsui, Y.; Yoshida, Y.; Tagawa, S.; Koe, J. R.; Fujiki, M. *J. Phys. Chem. B* **2002**, *106*, 6849−6852. (d) Seki, S.; Kunimi, Y.; Nishida, K.; Yoshida, Y.; Tagawa, S. *J. Phys. Chem. B* **2001**, *105*, 900−904. (e) Fratiloiu, S.; Grozema, F. C.; Koizumi, Y.; Seki, S.; Saeki, A.; Tagawa, S.; Dudek, S. P.; Siebbeles, L. P. A. *J. Phys. Chem. B* **2006**, *100*, 5984−5993.

(31) Battino, R. *Solubility Data Series: Volume 7, Oxygen and Ozone*; Pergamon Press: Oxford, England, 1981.

(32) (a) Tsubomura, H.; Mulliken, R. S. *J. Am. Chem. Soc.* **1960**, *82*, 5866−5974. (b) Scurlock, R. D.; Ogilby, P. R. *J. Phys. Chem.* **1989**, *93*, 5493−5500. (c) Kuriyama, Y.; Ogilby, P. R.; Mikkelson, K. V. *J. Phys. Chem.* **1989**, *98*, 11918−11923.

(33) Casanovas, J.; Grob, R.; Blanc, D.; Brunet, G.; Mathieu, J. *J. Chem. Phys.* **1975**, *63*, 3673−3675.